www.sciencemag.org/cgi/content/full/1127344/DC1

Supporting Online Material for

Imaging Intracellular Fluorescent Proteins at Nanometer Resolution

Eric Betzig,* George H. Patterson, Rachid Sougrat, O. Wolf Lindwasser, Scott Olenych, Juan S. Bonifacino, Michael W. Davidson, Jennifer Lippincott-Schwartz, Harald F. Hess

*To whom correspondence should be addressed. E-mail: betzige@hhmi.org

Published 10 August 2006 on *Science* Express
DOI: 10.1126/science.1127344

This PDF file includes:

Supporting online material, Betzig, *et al.*, "Imaging Intracellular Fluorescent Proteins at Nanometer Resolution"

MATERIALS AND METHODS

1. Instrumentation

Central to the performance of photoactivated localization microscopy (PALM) is the precise localization of single fluorescent molecules. When such localization is performed by a least-squares fit of an assumed two-dimensional gaussian point spread function (PSF) to each single molecule image, the mean-squared position error is given by [1]:

$$(s_{x,y}{}^2)_m \approx \frac{s^2 + a^2/12}{N_m} + \frac{4\sqrt{p}\,s^3 b_m{}^2}{a N_m{}^2} \qquad (1)$$

where s is the standard deviation of the PSF, a is the pixel size in the image (taking into account the system magnification), N_m is the total number of photons measured from molecule m, and b_m is the number of background photons collected in the fitting window used for molecule m. Therefore, PALM design is predicated on achieving the highest possible diffraction limited resolution (*i.e.*, small s) and collection efficiency (high N_m) consistent with minimal background noise b_m.

The instrument used to this end is shown schematically in Fig. S1. For continuous excitation of activated fluorescent proteins, light from a 10mW, $l_{exc} = 561\,\text{nm}$ diode pumped solid-state laser (Lasos GMBH, Jena, Germany) is fiber-coupled to an excitation collimator (EC, Fig. S1a), creating an excitation input beam (EIB) focused at the rear pupil plane internal to a 60X, 1.45NA total internal reflection fluorescence (TIRF) oil immersion objective (OBJ, Olympus America, Melville, NY). A narrow bandwidth laser line filter (EF, Semrock Inc., Rochester, NY) is used to reject both emission noise from the laser and autofluorescence generated in the optical path prior to the objective. For pulsed activation of the fluorescent proteins, a second diode laser (Coherent Inc., Santa Clara, CA), yielding up to 50mW at $l_{act} = 405\,\text{nm}$, is fiber-coupled through an intermediate galvanometer-based switch to an activation collimator (AC), creating a focused activation input beam (AIB) that is similarly bandpass filtered (AF, CVI Optical,

Covina, CA) before being combined with the excitation input beam at a dichroic mirror (DM, Semrock Inc.). This combined input beam (CIB) is then reflected from an elliptical spot on a custom-patterned, aluminized mirror (SM, Reynard Corp., San Clemente, CA) into the objective at a radius $(n_{sample} / NA) * 4.35 \approx 4.14 \text{ mm} \le r \le 4.35 \text{ mm}$ (for $n_{sample} \approx 1.38$) such that the resulting refracted ray transverses the low autofluorescence immersion oil (Cargille type FF, Structure Probe Inc., West Chester, PA) and is incident at the sample / cover slip (CS, #2 thickness, Fisher Scientific, Hampton, NH) interface at greater than the critical angle $q_c \approx \sin^{-1}(n_{sample} / n_{coverslip})$ for total internal reflection (TIR). An evanescent field is thereby established within the sample, exciting only those molecules within its nanometric decay length. Virtually all the incident energy of the excitation and activation beams, however, is reflected at the interface to yield a combined output beam (COB) emerging from the objective, which is reflected from a second elliptical spot on mirror SM diagonally opposite the first. This beam is then divided at dichroic mirror DM into separate excitation and activation output beams (EOB, AOB) that are finally directed to respective beam dumps.

It should be noted that an additional advantage of the TIRF geometry is that the emitted photons travel only sub-wavelength distances within the sample, and thus are largely unaffected by wavefront aberrations that might otherwise result in an offset between each molecule and its center of fluorescence emission.

For typical molecular cross-sections ($: 10^{-16} \text{cm}^2$), the reflected excitation beam energy may be 10^{15}-fold more intense than the molecular signal beam (ASB, Fig. S1b) emerging from the objective. Therefore, a key challenge in this through-the-objective TIRF geometry is to isolate the molecular signal with maximum efficiency from both the interface-reflected excitation beam and any autofluorescence generated by this beam in the optics encountered thereafter. The custom mirror SM used here is substantially more effective than the dichroic type mirror traditionally used for this purpose. The mirror has an elliptical, anti-reflection coated, transmissive aperture whose projection perpendicular to the objective axis matches the 8.7 mm diameter of the rear pupil, and therefore passes signal beam ASB to the detection optics with high efficiency. More importantly, for an elliptical reflective spot D times larger than the gaussian width of the reflected beam at the spot, only ~erfc(D) of the excitation energy is passed onto the detection optics, or $\sim 2 \cdot 10^{-5}$ to $\sim 2 \cdot 10^{-8}$ for D = 3 or 4, respectively. Furthermore, since the spots occlude

only a small fraction of the periphery of the rear pupil (for 1mm diameter spots, ~13% of the outer 1 mm annular area, or 5% of the total rear pupil area), they insignificantly degrade the detection numerical aperture and thus the PSF standard deviation *s* critical to accurate localization. Lastly, unlike a dichroic mirror, the custom mirror is wavelength insensitive, and therefore can be used with different excitation lasers and photoactivatable fluorescent proteins (PA-FPs) without replacement. Although only two spots were used in these experiments, the mirror includes four for eventual multi-angle, multi-polarization and/or standing wave TIRF excitation.

With this excitation geometry, a round, gaussian beam emerging from a collimator produces a round, gaussian beam in the plane of the sample / cover slip interface, since a $\cos q$ factor from the projection of the collimator beam on the spherical wavefront produced by the objective is canceled by a $\cos q$ factor from the oblique angle of incidence of the resulting focused beam at the interface. Collimator lenses of 3, 6, and 9 mm focal length are used interchangeably to produce excitation fields of $1/e^2$ diameter ~23, 49, and 77 μm, respectively, at the interface: the former when excitation intensity and hence imaging speed is paramount, and the latter when a larger field of view is desired. Typically, 0.5-2.0 mW of excitation power is delivered to the rear pupil of the objective, and anywhere from 40 μW to 4.0 mW of activation power. Furthermore, as the population of inactivated PA-FPs is depleted, the activation power is commonly increased exponentially to maintain an approximately constant density of activated PA-FPs in every frame.

After passage through custom spotted mirror SM, the largely collimated signal beam ASB emerging from the infinity-corrected objective OBJ is reflected by a first mirror (MR, Fig. S1b) to travel along the axis of the detection optics. Any remaining excitation light (as well as much of the remaining activation light) traveling substantially along this axis is then removed by a Raman edge filter (RF, Semrock Inc.). However, because the optical density of this filter decreases rapidly with increasing deviation from normal incidence, baffles (BF) are placed on either side of the filter to remove scattered light at higher angles of incidence generated elsewhere within the system. The filtered signal beam is then focused (FSB) with an acromatic tube lens (TL, Edmund Optics, Barrington, NJ) onto the face of a back-illuminated, thermoelectrically cooled (-50°C), electron multiplying CCD camera (CCD, Andor Scientific, South Windsor, CT) to create the

desired image of isolated single molecules. A 405 nm notch filter (NF, Semrock Inc.) is also included to further insure that the camera is not saturated when the activation beam is applied.

Analysis of Eq. 1 reveals that, in the presence of non-negligible background noise (e.g., detector dark noise, autofluorescence, and emission from inactive PA-FPs), the optimum pixel size a for accurate localization is one comparable to the standard deviation s of the PSF [1]. At the 1.45NA of the objective, this condition is approximately satisfied by choosing a tube lens of 400 mm focal length, yielding: a 133X magnified image at the CCD; a 120 nm effective pixel size; and a maximum field of view of 61 x 61 μm. To provide a wider field of view during periodic realignments of the system, the 400 mm lens is replaced by one of 200 mm focal length, and the beam is diverted to an eyepiece for direct viewing.

For most samples, the largest background initially appears at the features of interest in the sample itself – presumably due to weak emission from the large population of weakly emitting, still inactive PA-FPs. Therefore, standard commercial #2 cover slips were deemed adequate for the experiments described here. However, for samples with far fewer PA-FPs, or samples in which most of the PA-FPs have been bleached, cover slip autofluorescence becomes the dominant background source. Preliminary experiments have indicated that ~5x less autofluorescence exists in fused silica cover slips (Structured Probe Inc.).

With the 10mW excitation laser used thus far, a complete image stack yielding a single PALM image takes several hours to nearly a day to generate. The instrument therefore should be dimensionally stable to at least the desired level of PALM resolution over such time scales. Concerns that such stability would be hard to achieve in a commercial microscope led to the decision to build our initial PALM prototype in a compact, custom microscope head (Fig. S1c) designed to maximize mechanical stability and minimize thermal drift. Borrowing from the design concepts of scanning probe microscopy, a cylindrically symmetric main tube (MT) joins the objective to the sample holder (SH) / cover slip over the shortest, and hence most stiff, possible path. The sample holder has a top opening to allow different liquid media to be introduced at the sample, and is mounted in an plate (XY) for lateral xy translation relative to the objective with two ¼-80 adjustment screws and corresponding opposed spring loaded plungers

(screws and plungers not shown). Two or four springs (PS) are used to preload this plate against three additional ¼-80 screws (ZS), which provide the necessary vertical focus adjustment. Also shown are the collimator adjustment screws (CA) that are used to control the positions and angles at which the excitation and activation beams enter the objective rear pupil.

With these precautions, sample drift was often contained to within ~50 nm or less over the course of acquiring a complete image stack (Fig. S2). The PALM images in Figs. 2 and 4 were obtained using image stacks or portions thereof for which the position was particularly stable. Fig. 3 and other more recent images were acquired while simultaneously tracking single luminescent beads added sparsely to the sample (e.g., quantum dots or 50 nm gold beads (Microspheres-Nanospheres, Mahopac, NY)), and correcting for the drift thereby measured (Fig. S2) during the post-acquisition analysis. Such fiducial-based drift compensation may also permit the adaptation of PALM to commercial microscopes, allowing the investigation of samples at various magnifications and under a variety of established imaging modalities (e.g., DIC) in addition to PALM.

2. Sample Preparation

Cover Slip Preparation

In order to remove fluorescent surface contamination, round 18 mm #2 cover slips (Fisher Scientific, Pittsburgh, PA) were cleaned by sonication in 1% hydrofluoric acid for 5 minutes at room temperature. The cover slips were rinsed 10-20 times with distilled H_2O. Cover glasses were stored in distilled H_2O until use. Immediately prior to use, the cover slips were placed 100% ethanol and rinsed three times with sterile distilled H_2O.

Cell Culture

COS 7 cells (Figs. 2, 3, 4e,and 4f) were grown in Dulbecco's Modified Eagle Media (DMEM) containing 10% fetal bovine serum (FBS), 2 mM glutamine (all from Biosource International, Rockville, MD). Cover slips (see above) were placed in 35 mm cell culture dishes (Corning Incorporated, Corning. NY) and cells grown overnight at 37°C before transfection using FuGENE 6 transfection reagent (Roche, Indianapolis, IN). Cells were fixed with 4% paraformaldehyde and 0.5% glutaraldehyde (Electron Microscopy

Sciences, Hatfield, PA) in PBS for 20 minutes, washed 3-5 times with PBS, and stored in PBS until imaging.

FoLu (grey fox lung fibroblasts; ATCC CCL-168) cells (Figs. 4a-4d) were cultured in a 50:50 mixture of Ham's F-10 and DMEM media supplemented with 12.5% Cosmic calf serum (Hyclone). Cells were grown directly on 18-mm cover slips. In transient transfections, cultures were treated with the appropriate DNA vector in either Lipofectamine 2000 (Invitrogen) or Effectene (Qiagen) at 50-70% confluence according to the manufacturer's guidelines. After transfection, the cultures were allowed to express the fusion product for at least 48 hours prior to fixation. Adherent cells on cover slips were fixed with freshly-prepared 4% paraformaldehyde in phosphate buffered saline (PBS) for 10 minutes followed by several 5-minute washes with PBS. Cells for sectioning were fixed with a mixture of 4% paraformaldehyde and 0.5% glutaraldehyde for 10 minutes and washed 2x for 10 minutes with 50 mM glycine in PBS. FoLu cells were chosen because of their sharply defined actin stress fibers and numerous focal adhesions at the cellular periphery.

For Figs. 4e, 4f, COS7 cells grown on cover slips were transiently transfected for dEos-tagged Gag expression using Lipofectamine 2000 (Invitrogen) according to the manufacturer's instructions. Cells were briefly fixed in 3.7% formaldehyde 24 hours thereafter.

Plasmid Construction

Plasmids were constructed for expression of the PA FPs in bacteria for protein purification and for expression as chimeras in mammalian cells. The bacterial expression plasmids for the other PA FPs were constructed by subcloning the complimentary DNAs (cDNAs) in frame with an N-terminal 6X histidine tag of the pRSETA (Invitrogen) using the BamHI and EcoRI restriction endonuclease sites. The mammalian expression plasmids were constructed by subcloning the complimentary DNAs (cDNAs) into the pEGFP-N1, pEGFP-C1, and pEGFP-C2 plasmids from which the EGFP cDNA was removed by restriction endonuclease digestion. The details and primers are listed below:

pRSETA bacteria expression plasmids -- The mEosFP [2] cDNA was amplified from the plasmid, pcDNA3-Flag1 EosFP T158H/V123T (gift from Dr. Jorg Wiedenmann), using the N-terminal primer 5'-

GATCGGATCCATGAGTGCGATTAAG-3’ containing a BamHI site (underlined) and the C-terminal primer 5’-GATCGAATTCTTATCGTCTGGCATTGTC-3’ containing an EcoRI site (underlined).

The dEosFP(insert EosFP reference) cDNA was amplified from the plasmid, pcDNA3-Flag1 EosFP T158H (gift from Dr. Jorg Wiedenmann), using the N-terminal primer 5’-GATCGGATCCATGAGTGCGATTAAG-3’ containing a BamHI site (underlined) and the C-terminal primer 5’-GATCGAATTCTTATCGTCTGGCATTGTC-3’ containing an EcoRI site (underlined).

The Kaede [3] cDNA was amplified from the plasmid, pKaede-MN1 (MBL Medical and Biological Laboratories Co., Ltd., Naka-ku Nagoya, Japan) using the N-terminal primer 5’-GACGGATCCATGAGTCTGATTAAAC-3’ containing a BamHI site (underlined) and the C-terminal primer 5’-GACGAATTCTTACTTGACGTTGTC-3’ containing an EcoRI site (underlined).

The KiKGR [4] cDNA was amplified from the plasmid, Kikume Green-Red (pKiKGR1-MN1) (MBL Medical and Biological Laboratories Co., Ltd., Naka-ku Nagoya, Japan) using the N-terminal primer 5’-GACGGATCCATGAGTGTGATTAC-3’ containing a BamHI site (underlined) and the C-terminal primer 5’-GACGAATTCTTACTTGGCCAGCC-3’ containing an EcoRI site (underlined).

The amplification products were gel purified, digested with the restriction endonucleases, BamHI and EcoRI, and ligated into a similarly digested pRSETA (Invitrogen) to produce the pRSETA -mEosFP, pRSETA -dEosFP, pRSETA -Kaede, and pRSETA -KikGR, respectively.

N1 plasmids -- The mEosFP cDNA was amplified from the plasmid, pcDNA3-Flag1 EosFP T158H/V123T (gift from Dr. Jorg Wiedenmann), using the N-terminal primer 5’-GATCGGATCCACCGGTCGCCACCATGAGTGCGATTAAG-3’ containing a BamHI site (underlined) and the C-terminal primer 5’-GATCCGCGGCCGCTTTATCGTCTGGCATT-3’ containing a NotI site (underlined).

The dEosFP cDNA was amplified from the plasmid, pcDNA3-Flag1 EosFP T158H (gift from Dr. Jorg Wiedenmann), using the N-terminal primer 5’-GATCGGATCCACCGGTCGCCACCATGAGTGCGATTAAG-3’ containing a BamHI site (underlined) and the C-terminal primer 5’-GATCCGCGGCCGCTTTATCGTCTGGCATT-3’ containing a NotI site (underlined).

The Kaede cDNA was amplified from the plasmid, pKaede-MN1 (MBL Medical and Biological Laboratories Co., Ltd., Naka-ku Nagoya, Japan), using the N-terminal primer 5'-GATCGGATCCACCGGTCGCCACCATGAGTCTGATTAAAC-3' containing a BamHI site (underlined) and the C-terminal primer 5'-GATCCGCGGCCGCTTTACTTGACGTTGTC-3' containing a NotI site (underlined).

The KiKGR cDNA was amplified from the plasmid, Kikume Green-Red (pKiKGR1-MN1) (MBL Medical and Biological Laboratories Co., Ltd., Naka-ku Nagoya, Japan), using the N-terminal primer 5'-GATCGGATCCACCGGTCGCCACCATGAGTGTGATTAC-3' containing a BamHI site (underlined) and the C-terminal primer 5'-GATCCGCGGCCGCTTTACTTGGCCAGCC-3' containing a NotI site (underlined).

The amplification products were gel purified, digested with the restriction endonucleases, BamHI and NotI, and ligated into a similarly digested pEGFP-N1 (Clontech Laboratories, Inc., Palo, Alto, CA) to produce the mEosFP-N1, dEosFP-N1, Kaede-N1, and KikGR-N1, respectively.

C1 plasmids -- The mEosFP cDNA was amplified from the plasmid, pcDNA3-Flag1 EosFP T158H/V123T (gift from Dr. Jorg Wiedenmann), using the N-terminal primer 5'-GATCACCGGTCGCCACCATGAGTGCGATTAAG-3' containing an AgeI site (underlined) and the C-terminal primer 5'-GATCCTCGAGATCTGAGTCCGGATCGTCTGGCATTGTC-3' containing an XhoI site (underlined).

The dEosFP cDNA was amplified from the plasmid, pcDNA3-Flag1 EosFP T158H (gift from Dr. Jorg Wiedenmann), using the N-terminal primer 5'-GATCACCGGTCGCCACCATGAGTGCGATTAAG-3' containing an AgeI site (underlined) and the C-terminal primer 5'-GATCCTCGAGATCTGAGTCCGGATCGTCTGGCATTGTC-3' containing an XhoI site (underlined).

The Kaede cDNA was amplified from the plasmid, pKaede-MN1 (MBL Medical and Biological Laboratories Co., Ltd., Naka-ku Nagoya, Japan), using the N-terminal primer 5'-GATCGGATCCACCGGTCGCCACCATGAGTCTGATTAAAC-3' containing an AgeI site (underlined) and the C-terminal primer 5'-

GATCCTCGAGATCTGAGTCCGGACTTGACGTTGTCCGG-3’ containing an XhoI site (underlined).

The KiKGR cDNA was amplified from the plasmid, Kikume Green-Red (pKiKGR1-MN1) (MBL Medical and Biological Laboratories Co., Ltd., Naka-ku Nagoya, Japan), using the N-terminal primer 5’-GATCGGATCCACCGGTCGCCACCATGAGTGTGATTAC-3’ containing an AgeI site (underlined) and the C-terminal primer 5’-GATCCTCGAGATCTGAGTCCGGACTTGGCCAGCCTTGG-3’ containing an XhoI site (underlined).

The amplification products were gel purified, digested with the restriction endonucleases, AgeI and XhoI, and ligated into a similarly digested pEGFP-C1 (Clontech Laboratories, Inc., Palo, Alto, CA) to produce the mEosFP-C1, dEosFP-C1, Kaede-C1, and KikGR-C1, respectively.

C2 plasmids -- The mEosFP cDNA was amplified from the plasmid, pcDNA3-Flag1 EosFP T158H/V123T (gift from Dr. Jorg Wiedenmann), using the N-terminal primer 5’-GATCACCGGTCGCCACCATGAGTGCGATTAAG-3’ containing an AgeI site (underlined) and the C-terminal primer 5’-GATCCTCGAGATCTGAGTCCGGCCGGATCGTCTGGCATTGTC-3’ containing an XhoI site (underlined).

The dEosFP cDNA was amplified from the plasmid, pcDNA3-Flag1 EosFP T158H (gift from Dr. Jorg Wiedenmann), using the N-terminal primer 5’-GATCACCGGTCGCCACCATGAGTGCGATTAAG-3’ containing an AgeI site (underlined) and the C-terminal primer 5’-GATCCTCGAGATCTGAGTCCGGCCGGATCGTCTGGCATTGTC-3’ containing an XhoI site (underlined).

The Kaede cDNA was amplified from the plasmid, pKaede-MN1 (MBL Medical and Biological Laboratories Co., Ltd., Naka-ku Nagoya, Japan), using the N-terminal primer 5’-GATCGGATCCACCGGTCGCCACCATGAGTCTGATTAAAC-3’ containing an AgeI site (underlined) and the C-terminal primer 5’-GATCCTCGAGATCTGAGTCCGGCCGGACTTGACGTTGTCCGG-3’ containing an XhoI site (underlined).

The KiKGR cDNA was amplified from the plasmid, Kikume Green-Red (pKiKGR1-MN1) (MBL Medical and Biological Laboratories Co., Ltd., Naka-ku Nagoya, Japan), using the N-terminal primer 5'-GATCGGATCCACCGGTCGCCACCATGAGTGTGATTAC-3' containing an AgeI site (underlined) and the C-terminal primer 5-GATCCTCGAGATCTGAGTCCGGCCGGACTTGGCCAGCCTTGG-3' containing an XhoI site (underlined).

The amplification products were gel purified, digested with the restriction endonucleases, AgeI and XhoI, and ligated into a similarly digested pEGFP-C2 (Clontech Laboratories, Inc., Palo, Alto, CA) to produce the mEosFP-C2, dEosFP-C2, Kaede-C2, and KikGR-C2, respectively.

Chimeric Proteins Mammalian Expression Plasmids

To produce the PA-FP-tagged CD63 (Fig. 2), the oligonucleotide, 5'-GAATTCGGCTCCACCGGCTCCACCGGCTCCACCGGCGCGGATCC-3', containing restriction sites for EcoRI and BamHI (underlined, respectively) was cloned into pEGFP-N1. This generated a plasmid containing repetitive sequence of serine, threonine, and glycine as an additional 10 amino acid linker N-terminal to EGFP denoted pEGFP-NL. The CD63 was amplified by polymerase chain reaction using the N-terminal primer, 5'-GATCCTCGAGCGCCACCATGGCGGTGGAAGGAG-3', containing an XhoI site (underlined) and the C-terminal primer, 5'-GATCGAATTCCGACATCACCTCGTAGC-3', containing an EcoRI restriction site (underlined) using pEGFP-C2-CD63 (gift from Dr. Juan Bonifacino and Dr. Robert Lodge, Cell Biology Metabolism Branch, NICHD, NIH, Bethesda, MD) as template. The amplification product was gel purified, digested with the restriction endonucleases, XhoI and EcoRI, and ligated into a similarly digested pEGFP-NL to produce pEGFP-NL-CD63 expression plasmid. The CD63-NL cDNA was removed from this plasmid by digestion with the endonucleases, XhoI and BamHI, and ligated into similarly digested mEosFP-N1, dEosFP-N1, Kaede-N1, and KikGR-N1 plasmids. These produced the mEosFP-NL-CD63, dEosFP-NL-CD63, Kaede-NL-CD63, and KikGR-NL-CD63, respectively.

To produce the dEos-tagged vinculin (Figs. 4a, 4b), the EcoRI site within the vinculin sequence of pKO-Vinculin was replaced with a silent in-frame mutation using site-directed mutagenesis (pmKO obtained from MBL). The resulting plasmid, pKO-VinculinRImut, was cut with NheI and EcoRI. The dEos coding region was amplified from pdEos/Actin using the forward primer 5'-GAACCGTCAGATCC GCTAGCACC-3' and the reverse primer, 5'-TATAGAATTCTCTCGTCTGGCATTGTCAGGCAATC-3', which introduced an EcoRI site into the resulting PCR product. The PCR product was digested with NheI and EcoRI and cloned in frame into the cut pKO-VinculinRImut plasmid.

To produce the tdEos-tagged actin (Figs. 4c, 4d), pEGFP/actin (human *beta*-actin; Clontech) was cut with NheI and XhoI. The dEos coding sequence was amplified from a plasmid kindly provided by J. Wiedenmann using the forward primer: 5'-TAGCTAGCACCATGGTGGCGATTAAGCCAGACATGAAGAT-3', and the reverse primer: 5'-CTGACTCGAGATCGTCTGGCATTGTCAGGC-3', which introduced a which introduced, NheI and XhoI sites, respectively, in the resulting PCR product. The digested PCR product was cloned in-frame into the cut pEGFP/actin vector.

To produce the dEos-tagged HIV-1 assembly protein Gag (Figs. 4e, 4f), a Rev-independent HXB2 Gag sequence was excised from pGagEGFP [6] (gift from Dr. Marilyn Resh, Memorial Sloan-Kettering Cancer Center, New York, NY, USA) by digestion with XhoI and BamHI. The resulting fragment was inserted in frame into the XhoI and BamHI sites of the dEosFP-N1 plasmid.

Protein Expression and Purification

All pRSET plasmids were transformed into the *Escherichia coli* strain, Epicurian Coli BL21 (DE3) pLysS (Stratagene, La Jolla, CA), for protein expression at 28°C. Starter cultures were grown overnight in terrific broth containing 100 µg/mL ampicillin and 25 µg/mL chloramphenicol at 37°C and used to inoculate 500 ml cultures. These were grown to 0.4-0.5 optical density at 600 nm, induced with 1 mM IPTG, and grown for 5 hours before harvesting by centrifugation. The cells were stored in sonication buffer(50mM Na_2HPO_4, 300mM NaCl) until purification was continued. After thawing, the cells were lysed by incubation with lysozyme followed by sonication. Insoluble debris was pelleted by centrifugation. The lysate was incubated with Ni NTA agarose

(Qiagen Inc., Valencia, CA) for 1 hour at room temperature. The resin was washed once with sonication buffer containing 10 mM imidazole and once with sonication buffer containing 25 mM imidazole. The proteins were eluted with sonication buffer using 100 mM imidazole. The proteins were dialyzed in Slide-A-Lyzer cassettes with 10,000 MWCO (Pierce Chemical Company, Rockford, IL) against phosphate-buffered saline (PBS) pH 7.4 to remove the imidazole. Protein concentrations were determined by BCA assay and the purities were determined by scanning densitometry of the fractions on coomassie-stained SDS gels.

Protein Biotinylation

Purified PA FPs (1 µM) were incubated with 13 µM biotinamido hexanoic acid 3-sulfo-N-hydroxysuccinide ester (BAC-SulfoNHS) (B 4430, Sigma, St. Louis, MO) in PBS pH 7.4 for 30 minutes at room temperature. The proteins were dialyzed in Slide-A-Lyzer cassettes with 10,000 MWCO (Pierce Chemical Company, Rockford, IL) against phosphate-buffered saline (PBS) pH 7.4 to remove the free BAC-SulfoNHS.

Single Molecule Immobilization on Cover Slips

Immediately prior to use, cleaned cover slips (see above) were rinsed with methanol and dried with compressed air. To immobilize the molecules, 5 µl of a1 mg/ml solution of biotin-BSA in PBS (A 8549, Sigma, St. Louis, MO) was placed in the center of the cover slip and incubated at room temperature for 5 minutes. The cover slip was then washed once and incubated with 5 µl of a 1 mg/ml solution of streptavidin in PBS (S 462, Sigma, St. Louis, MO) at its center at room temperature for 5 minutes. The cover slip then was washed once and incubated with 5 µl of biotinylated PA FP ranging in concentration from $1e^{-10}$ M to $1e^{-8}$ M at the center at room temperature for 5 minutes. Finally, the cover slip was washed once and placed in PBS until imaging.

Immunofluorescence for Characterization by Confocal Microscopy

Cells were fixed for 15 minutes with 4% paraformaldehyde (Electron Microscopy Sciences, Hatfield, PA) in PBS, washed three times with PBS containing 10% FBS and 50 mM glycine before incubating for 1 h at 25°C with 5 µg/ml monoclonal anti-GM130 (Transduction Laboratories, Lexington, KY) in PBS containing 10% FBS and 0.1%

saponin or 8 µg/ml monoclonal anti-lamp-2 (H4B4, Developmental Studies Hybridoma Bank, Iowa City, IA) in PBS containing 10% FBS and 0.1% saponin. Cells were again washed three times with PBS containing 10% FBS before a 1 h incubation with 4 µg/ml goat anti-mouse IgG labeled with Alexa Fluor 633 (Molecular Probes, Inc. Eugene, OR) in PBS containing10%FBS and 0.1% saponin. The cells were washed three times with PBS containing 10% FBS before mounting in Fluoromount G (Southern Biotechnology Associates, Inc., Birmingham, AL).

Cryo-sectioning for PALM

Transfected cells were fixed 15 min. in PBS buffer pH 7.4 containing 0.1% glutaraldehyde and 4% paraformaldehyde and rinsed in PBS. Cells were incubated 15 min in PBS / Glycine 50mM, scraped in PBS / BSA 1%, embedded in 10 % Gelatine and infiltrated with sucrose 2.3 M. Thin cryo-sections were cut on a Reichter-E ultramicrotome, and collected on a glass cover slip.

3. Sample Characterization

Confocal Microscopy

Imaging was performed on either an Olympus Fluoview FV1000 (Tokyo, Japan) or Zeiss LSM510 laser scanning confocal microscope (Carl Zeiss, Thornwood, NY). Imaging on the Olympus microscope was performed with a 60X Plan Apochromat 1.4 NA objective and a 488/543/633 dichroic mirror. The green (non-activated) fluorescence of the PA FPs was imaged the 488 nm line of an argon ion laser and emission was collected over the range of 505-530 nm. The red (activated) fluorescence of the PA FPs was imaged with the 543 nm line of a HeNe laser and emission was collected over the range of 560-660 nm. Imaging on the Zeiss microscope was performed in multi-tracking mode on a with a 63X Plan Apochromat 1.4 NA objective and a 488/543/633 dichroic mirror. The green (non-activated) fluorescence of the PA FPs was imaged the 488 nm line of an argon ion laser and emission was collected with a BP505-550 filter. The Alexa Fluor 633 was imaged with the 633 nm line of a HeNe laser and emission was collected with LP650 nm filter.

Electron Microscopy

Cells were fixed in 2.5% glutaraldehyde in sodium cacodylate buffer, rinsed and post fixed 1h at room temperature in reduced osmium (1:1 mixture of 2% aqueous potassium ferrocyanide) as described previously [7]. After post fixation the cells were pre-embedded in Agar 2%, dehydrated in ethanol and processed for Epon embedding. Thin section were cut on a Reichter-E ultramicrotome, collected on copper grids and stained with lead citrate for 2 min. Sections were then examined with a CM 10 Philips electron microscope at 80kV.

Correlative Electron Microscopy

50-70 nm cryo sections were collected on copper grids coated with formvar/carbon and processed as described previously [8]. Briefly, after the PALM imaging the sections were rinced with PBS buffer, fixed with 1% glutaraldehyde for 10 min, stained with 3 % uranyl acetate for 10 min and covered with a methyl cellulose film.

4. PALM Data Acquistion

Cover slip mounted sections or cultured cells were placed in the sample holder of the PALM instrument (SH, Fig. S1) and brought to the focal plane of the oil-immersion TIRF objective with the ¼-80 *z*-adjustment screws (ZS, Fig. S1). For cultured cells and biotinylated single molecules, additional PBS was added to the sample chamber after sample insertion. Both brightfield (under broadband incandescent illumination) and conventional TIRF imaging (using the $l_{exc} = 561\,\text{nm}$ excitation laser) were used to translate laterally until a region of biological interest could be found. Because expression levels of PA-FP-tagged protein varied greatly from cell to cell, the selected region was then exposed to a brief (~1 s) pulse from the $l_{act} = 405\,\text{nm}$ activation laser. Only those regions exhibiting a large increase in fluorescence thereafter were chosen for PALM imaging.

Excitation power in the range of 0.2-2.0 mW at the rear pupil of the objective was applied continuously during the acquisition of each image stack, and focused to a circular region of $1/e^2$ diameter ~23, 49, and 77 μm (for excitation collimator lenses of focal length 3, 6, and 9 mm, respectively). Frame times t_{frame} for the single molecule images

comprising the stack therefore varied from 0.5 to 5.0 s. Specific times for Figs.2-4 are given in Table S1.

Activation power in the range of 0.04-4.0 mW at the rear pupil was applied in a brief pulse after acquisition of every F_{bleach} frames of the image stack. Values of F_{bleach} for Figs. 2-4 are given in Table S1. The pulse was controlled with a galvanometer-based switch computer-synchronized to the image acquisition trigger of the EMCCD camera. To maintain an approximately constant density of resolvable single molecules in the first frame after each activation pulse (even in the face of the depleting population of PA-FPs), the pulse was programmed to increase exponentially in duration (e.g., from 10ms to 1s) over the course of acquiring the complete image stack. The activation power was also manually adjusted on occasion to maintain an optimal molecular density.

Recently, quantum dots or 50 nm luminescent gold beads have been sparsely added to samples for PALM as fiducial marks to compensate for sample drift observed during data acquisition (Fig. S2). Individual dots are isolated and localized in the same manner as single PA-FPs.

5. Single Molecule Localization Algorithms

Molecular localization programs were written independently in two different programming environments: IDL (Research Systems, Inc., Boulder, CO, Figs. 1 and 3) and MATLAB (The MathWorks, Inc., Natick, MA, Figs. 2 and 4). Similar results were obtained in the two cases when applied to identical data. Details of the MATLAB code are given below.

The acquired data in the stack $D(x, y, f)$ of $f = 1\mathbf{K}\,F_{total}$ image frames is converted from EMCCD detector counts to photons after subtraction of a constant dark state offset. Starting at frame $f_n = F_{total} - 1$, a differential image $dD(x, y, f_n)/df$ = $D(x, y, f_n) - D(x, y, f_{n+1})$ is created, wherein molecules disappearing (i.e., bleaching or blinking off) between frames f_n and f_{n+1} appear as positive intensity peaks. Each such positive peak is individually analyzed in a fit window centered at its maximum and having a radius $2.5s$, where s is the standard deviation of the expected PSF at the detector. The peak is deemed to represent a molecule *m* worth fitting if the total number of signal photons $n_m(f_n)$ across the fit window in $dD(x, y, f_n)/df$ is significantly greater

than (e.g., 5x) the shot noise $\sqrt{b_m}$ from the background b_m remaining in the fit window after the molecule bleaches or blinks off, as determined by the photons remaining across the window in $D(x, y, f_{n+1})$. The image $\{dD(x, y, f_n)/df\}_m^{window}$ of each selected peak in its centered fit window is then stored in a buffer, and replaced in $D(x, y, f_n)$ with the background from $D(x, y, f_{n+1})$ in this same window, so that if the molecule also exists in frame f_{n-1}, it will appear as a peak in the next differential image, $dD(x, y, f_{n-1})/df$. This process is then repeated frame by frame backwards to the beginning to identify and isolate the data from all significant peaks in the image stack

If the maxima of two peaks occur at the same pixel (± 1) in successive frames, they are considered to arise from same molecule, and their stored images are summed across their common fit window. If, however, the pixel-identical maxima occur in nearby but *not* successive frames, it is not known whether they arise from the same molecule (i.e., one that temporarily blinked off between the frames) or two distinct molecules. If the former, their signals should be summed so that higher localization precision is achieved. If the latter, their signals should be localized separately, or else an erroneous localization measurement will arise from their sum. Currently, a purely empirical standard is used: identically positioned peaks separated by three or fewer frames are deemed to arise from the same molecule. We continue to search for means to either suppress blinking in the PA-FPs or unambiguously distinguish blinking molecules from ones nearby in time and space, as such means could enhance PALM performance.

The image data in the fit window for each molecule *m*, summed across all frames in which it appears, is fitted using a nonlinear least squares algorithm (MATLAB function lsqnonlin, optimization toolbox) to an assumed cylindrically symmetric two-dimensional gaussian PSF:

$$PSF(x, y, A, w) = A\exp\{-[(x-x_o)^2 + (y-y_o)^2]/2w^2\} \qquad (2)$$

where x_o, y_o, A, and w are treated as free fitting parameters. This yields best-fit values x_{fit1}, y_{fit1}, A_{fit1}, and w_{fit1}. To reduce the effect of outlying data points on the fitted location, a second fit is then performed to the same function, except with the data $P_m(x_i, y_i)$ at each pixel in the fit window weighted by the inverse of the squared residual, i.e., by $[(P_m(x_i, y_i) - PSF(x_i, y_i, A_{fit1}, w_{fit1}))^2]^{-1}$, arising from the first fit. The values $x_m \equiv x_{fit2}$ and $y_m = y_{fit2}$ arising from this second, weighted fit are chosen as the coordinates of molecule *m*. To aid in deciding which molecules to include when

rendering the ultimate PALM image, $A_m = A_{fit2}$ and $w_m = w_{fit2}$ are also stored, as are c_m^2 (the sum of the final squared residuals), the background b_m across the fit window in the frame in which the molecule finally disappears, and the total signal N_m collected from the molecule in all frames.

6. PALM Image Rendering Algorithms

Image rendering programs were also written independently in IDL (Figs. 1 and 3) and MATLAB (Figs. 2 and 4). Similar results were obtained in the two cases when applied to identical data. Details of the Matlab code are given below.

Based on the parameters determined during localization, the position variance $(s_{x,y}^2)_m$ for each localized molecule is estimated according to Eq. (1), with the ideal standard deviation *s* replaced by the best-fit standard deviation w_m. A PALM image is then constructed using some subset of the total number M_{total} of localized molecules satisfying certain constraints, such as: $N_m > (N_m)_{\min}$ ($(N_m)_{\min} \sim 200$ typical); $c_m^2 < (c_m^2)_{\min}$; $(w_m)_{\min} < w_m < (w_m)_{\max}$ (w_m within ±30% of s, typical); and/or $(s_{x,y}^2)_m > (s_{x,y}^2)_{\min}$. Values of N_m and $(s_{x,y})_m$ in particular used for rendering the images in Figs. 2-4 are given in Table S1.

When rendering PALM images, the number of molecules M_{image} to be included in the final image must be balanced against these constraints, particularly the maximum localization error $(s_{x,y})_{\max}$. Including fewer, but brighter, molecules results in higher localization and crisper images, but at a reduced molecular density indicative of increasingly incomplete information about the spatial distribution of the target protein (Fig. S5). Values of $(s_{x,y})_{\max}$ and M_{image} for Figs. 2-4 are also given in Table S1. The final PALM image is generated in a new *xy* frame by representing each localized molecule satisfying the chosen constraints as a gaussian of standard deviation $(s_{x,y})_m$ (rather than the much larger standard deviation *s* of the original PSF), normalized to unit strength when integrated over all *xy* space, and centered at best-fit coordinates x_m, y_m. The superresolution image resulting from the sum of all such rendered molecules thus provides a probability density map where brightness is proportional to the likelihood that a PA-FP molecule can be found at a given location.

Because photobleaching is a stochastic process, and the localization precision is determined by the total number of detected photons per molecule prior to bleaching, some statistical variation is to be expected in PALM images of a given area. Even greater variability is introduced in the typical case where the expressed fraction of PA-FP-tagged target protein is small compared to that of the wild-type protein, since their mutual assembly into organized cellular structures is stochastic in nature. This effect is demonstrated by the two PALM images of the same sample in Fig. S9, constructed from two separate subsets of localized PA-FPs. On length scales where the number of localized molecules is high (Figs. S10a, S10b), these statistical effects tend to average out to yield very consistent results. However, at magnification sufficiently high where the individual localized molecules can be seen (Figs. S10c, S10c), statistical variability can become significant. This effect is not unique to PALM – any superresolution technique based on generating signal from labels bound to target molecules rather than from the target molecules themselves will exhibit such variability at sufficiently low labeling fraction and sufficiently high spatial resolution.

One remedy to these issues is to increase the fraction of labeled target protein within the cell. Unfortunately, even monomeric PA-FPs such as mEos are sufficiently large that they can significantly perturb cellular structure and function when expressed at high levels. Higher density labeling might be possible with smaller photoactivatable molecules, such as caged dyes (9). Indeed, we have recently demonstrated high resolution PALM imaging by uncaging such dyes at $l_{act} = 405$ nm (e.g., CMNB caged fluorescein (Invitrogen, catalog no. G-21061) and CMNCBZ caged rhodamine –dextran (Invitrogen, catalog no. D-34678), Fig. S10). A challenge that remains is to attach these dyes to target proteins at high labeling fractions, yet with high specificity and geometrically tight binding as well.

SUPPORTING REFERENCES

1. R.E. Thompson, D.R. Larson, W.W. Webb, *Biophys. J.* **82**, 2775 (2002).
2. J. Wiedenmann, *et al.*, *Proc. Natl. Acad. Sci. USA* **101**, 15905 (2004).
3. R. Ando, H. Hama, M. Yamamoto-Hino, H. Mizuno, A. Miyawaki, *Proc. Natl. Acad. Sci. USA* **99**, 12651 (2002).
4. H. Tsutsui, S. Karasawa, H. Shimizu, N. Nukina, A. Miyawaki, *EMBO Reports* **6**, 233 (2005).
5. N.B. Cole, *et al.*, *Science* **273**, 797 (1996).
6. Hermida-Matsumoto, L., Resh, M.D., *J. Virol.* **74** 8670 (2000).
7. M.J. Karmosky, *Proc. 11th Meeting, Am. Soc. Cell Biol.*, New Orleans, LA, Abstr. 284, p.146 (1971).
8. J.M. Robinson, T. Takizawa, A. Pombo, P.R.J. Cook. *Histochem Cytochem*. **49,** 803 (2001).
9. J.C. Politz, *Trends Cell Biol.* **9**, 284 (1999).

SUPPORTING TABLE

Table S1. Parameters of merit for the acquisition and analysis of the PALM images in Figs. 2-4 of the main text: t_{frame} = acquisition time for each frame of the image stack; F_{bleach} = number of frames between activation pulses; F_{total} = total number of acquired frames in the image stack; M_{total} = total number of molecules localized from the data in the image stack; $(s_{x,y})_{\max}$ = maximum acceptable position error for inclusion in the final image; M_{image} = number of localized molecules comprising the final image.

	t_{frame} (sec)	F_{bleach}	F_{total}	image size (μm)	M_{total}	$(s_{x,y})_{\max}$ (nm)	M_{image}
Fig. 2b	0.5	20	20000	7.20 x 7.20	44937	24	10858
Fig. 2c	0.5	20	20000	2.04 x 2.04	11859	24	2840
Fig.2d	0.5	20	20000	0.70 x 0.70	2834	36	1128
Fig. 3b	0.8	20	40000	6.60 x 6.60	79415	24	25606
Fig. 3e	0.8	10	40000	1.80 x 1.80	18072	24	5558
Fig. 4b	0.6	10	20000	2.40 x 2.40	12181	36	3304
Fig. 4d	0.5	20	50000	2.64 x 2.64	17134	26	5080
Fig. 4f	5.0	20	20000	15.4 x 15.4	248234	60	46470

SUPPORTING FIGURES

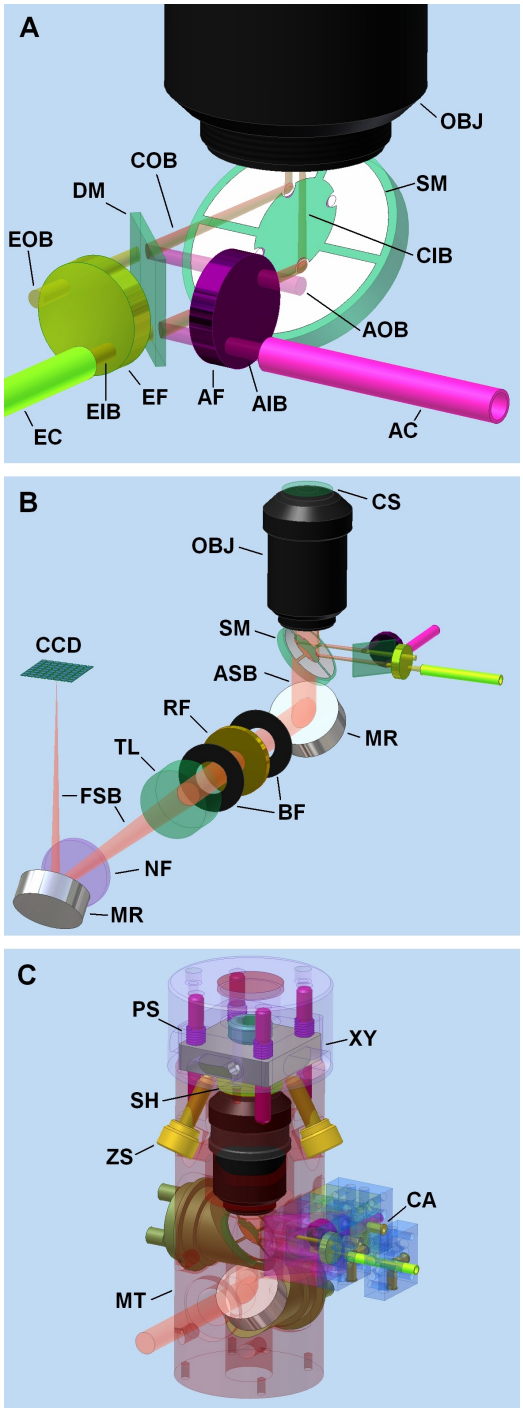

Fig. S1. Instrumentation for photoactivated localization microscopy (PALM). (**A**) Optical paths of the excitation and activation beams. (**B**) Optical path of the molecular signal beam to the EMCCD detector. (**C**) Other supporting elements of the microscope body. Labels are defined in Materials and Methods.

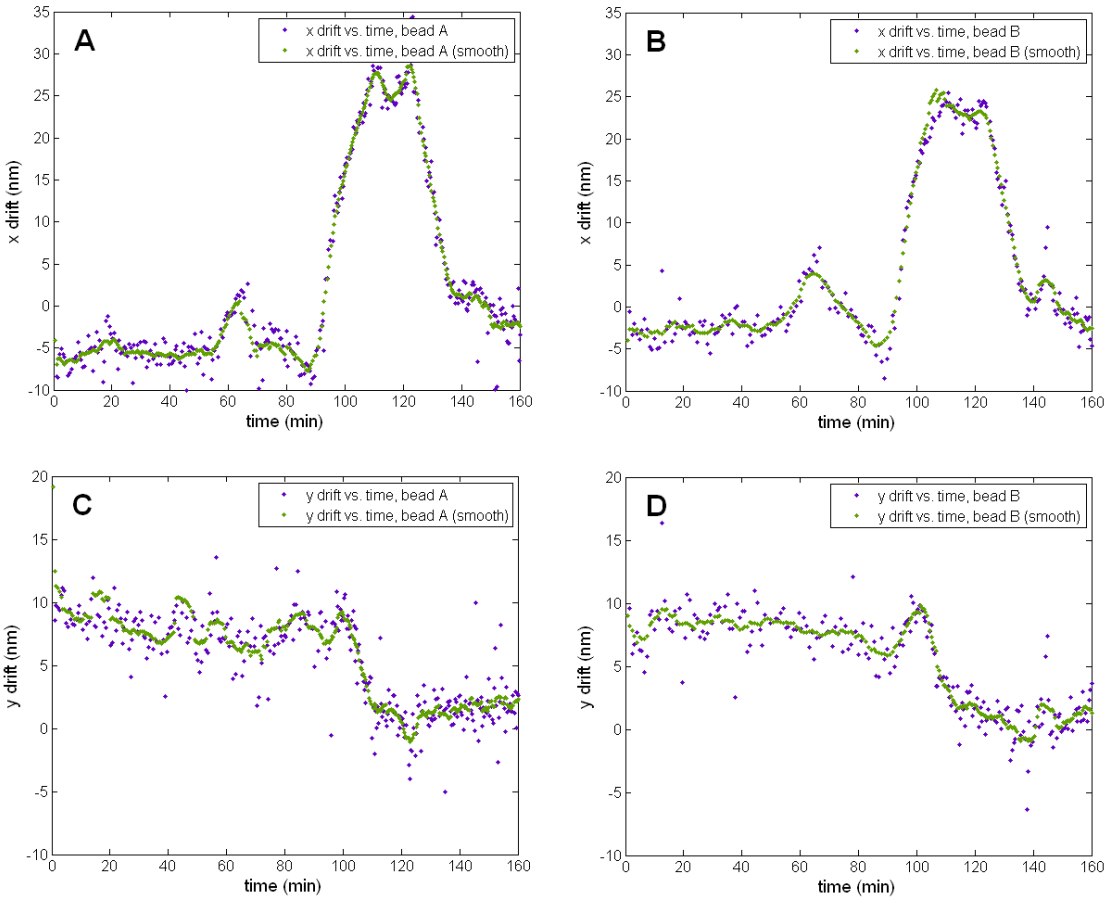

Fig. S2. Sample drift in the PALM instrument over >2.5 hours as measured simultaneously by two different 50 nm diameter luminescent gold beads. Each data point represents a localized position determined after collection of 40,000 signal photons. Open loop drift is often < 50 nm and, using such fiducial markers, the drift-based contribution to position errors in PALM data can be reduced to a few nanometers.

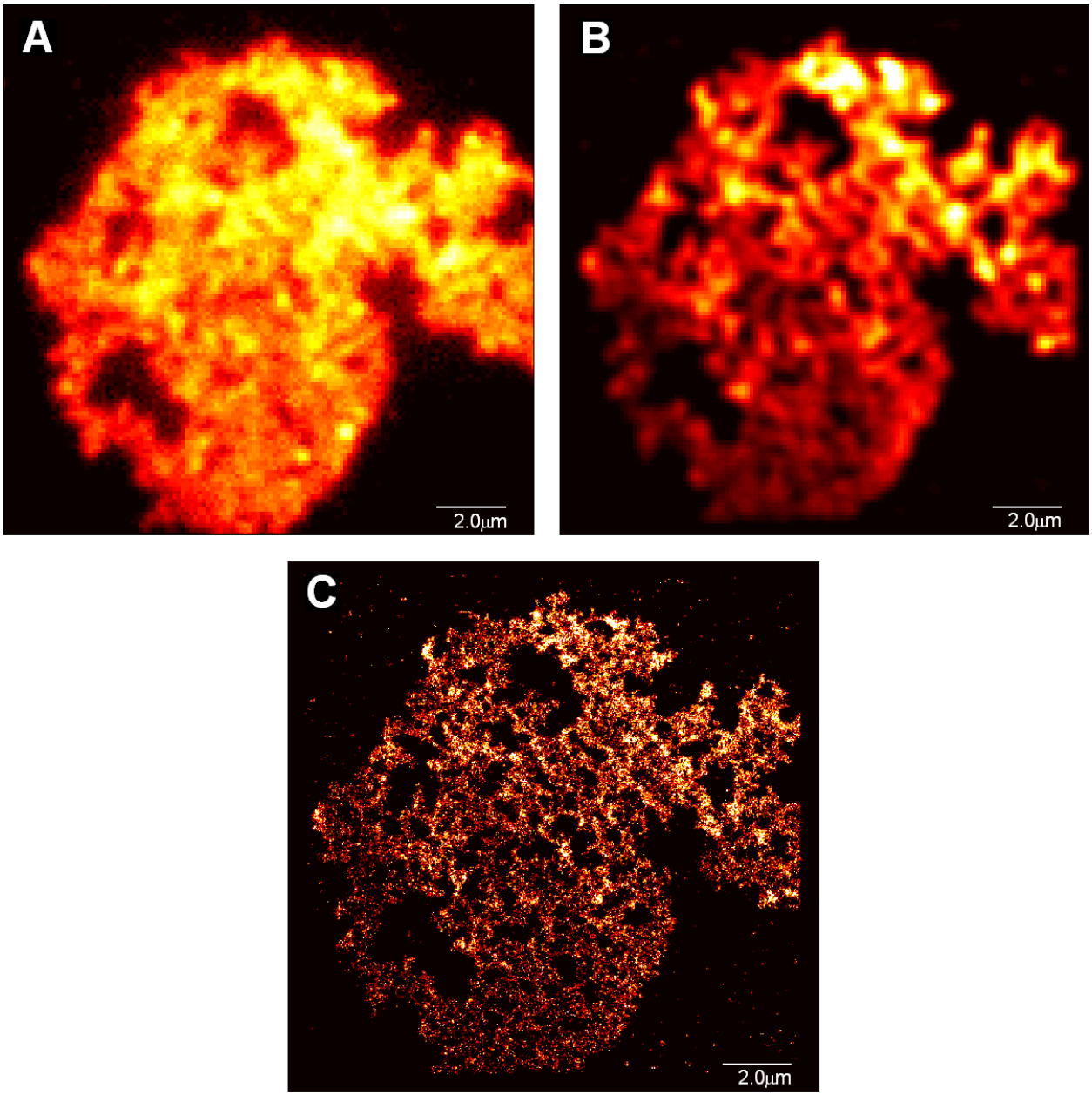

Fig. S3. Images of an aggregation of 50 nm diameter plain polystyrene beads with the PA-FP Kaede deposited thereon. (**A**) Conventional TIRF image obtained prior to PALM data acquisition, using $l_{exc} = 491$ nm excitation, and detection of l_{ems} **:** $500 - 550$ nm emission from inactivated (green state) molecules. (**B)** Summed TIRF image constructed by summing all the activated (red state), background-subtracted, diffraction-limited single molecule images in the entire PALM data stack. The diffraction-limited result (**B**) is similar to if somewhat more revealing than (**A**) -- the differences may be attributable to the molecule-by-molecule background subtraction employed in (**B**). (**C**) PALM image constructed by summing the position probability gaussians determined for all localized molecules in the data stack.

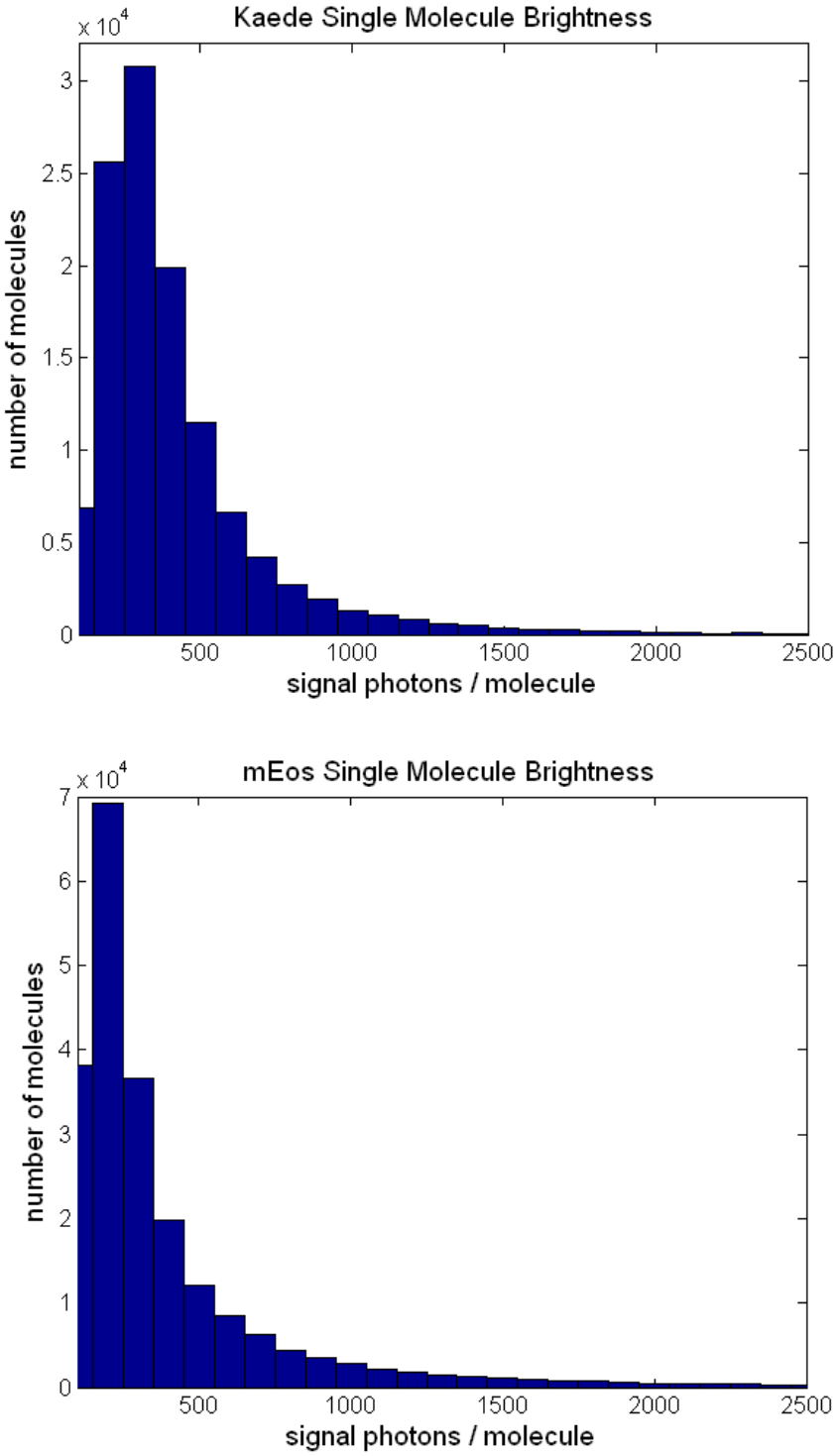

Fig. S4. Histograms of total number of photons detected for Kaede (top) and mEos (bottom) activated single molecules on a cover slip immersed in phosphate buffered saline. Note the shift of the Kaede histogram towards higher brightness.

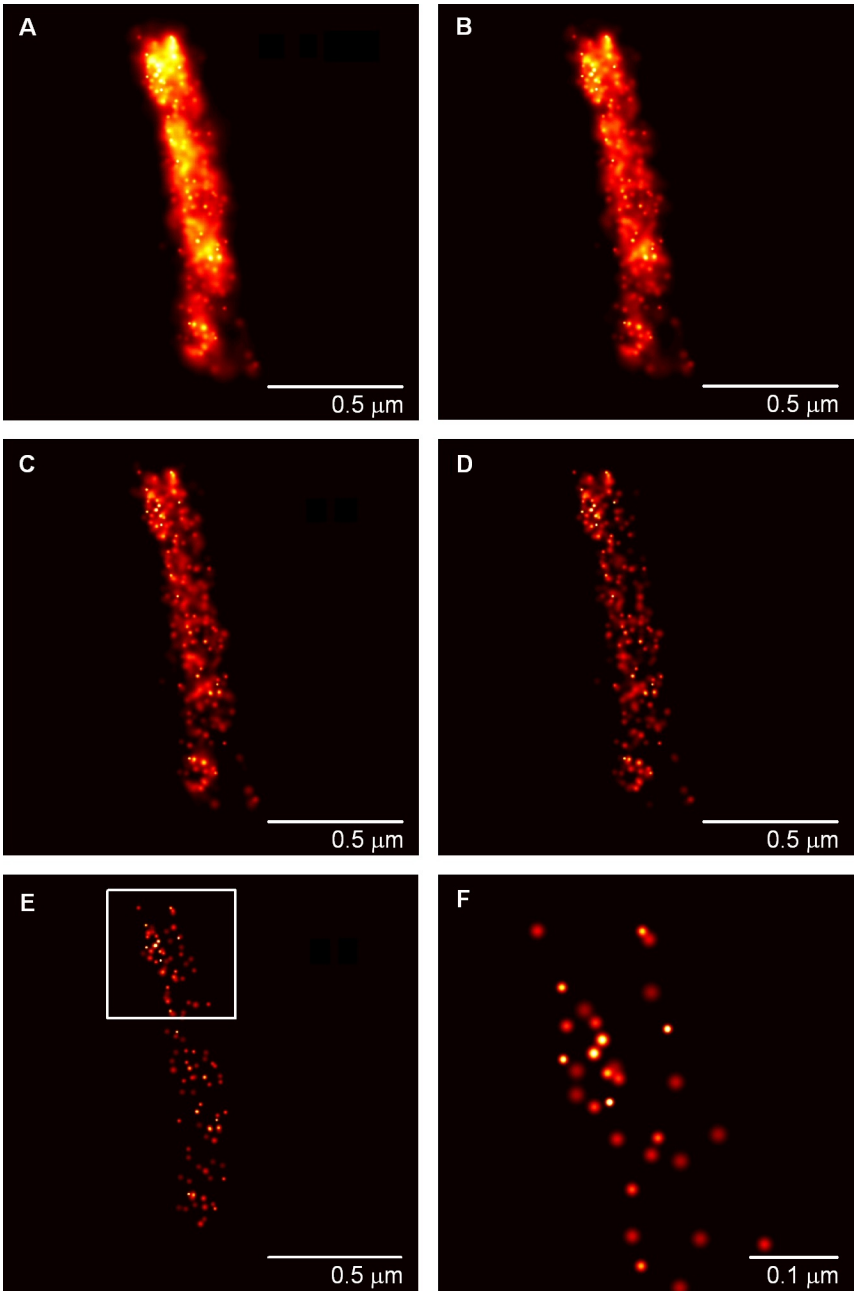

Fig. S5. Six PALM images of dEosFP-tagged cytochrome c oxidase within the lumen of a mitochondrion in a HeLa cell, generated from the same set of localized molecules, but with increasingly stringent constraint on the maximum position error $(s_{x,y})_{\max}$ allowed for the molecules comprising the image. Decreasing $(s_{x,y})_{\max}$ results in a crisper image, but with fewer included molecules M_{image}, and thus increasingly incomplete information on the spatial distribution of the target protein. (**A**) $(s_{x,y})_{\max} = 48$ nm, $M_{image} = 3037$; (**B**) $(s_{x,y})_{\max} = 36$ nm, $M_{image} = 1747$; (**C**) $(s_{x,y})_{\max} = 24$ nm, $M_{image} = 769$; (**D**) $(s_{x,y})_{\max} = 18$ nm, $M_{image} = 406$; (**E**) $(s_{x,y})_{\max} = 12$ nm, $M_{image} = 137$; (**F**) (sub-region indicated in (**E**)) $(s_{x,y})_{\max} = 9.0$ nm, $M_{image} = 33$.

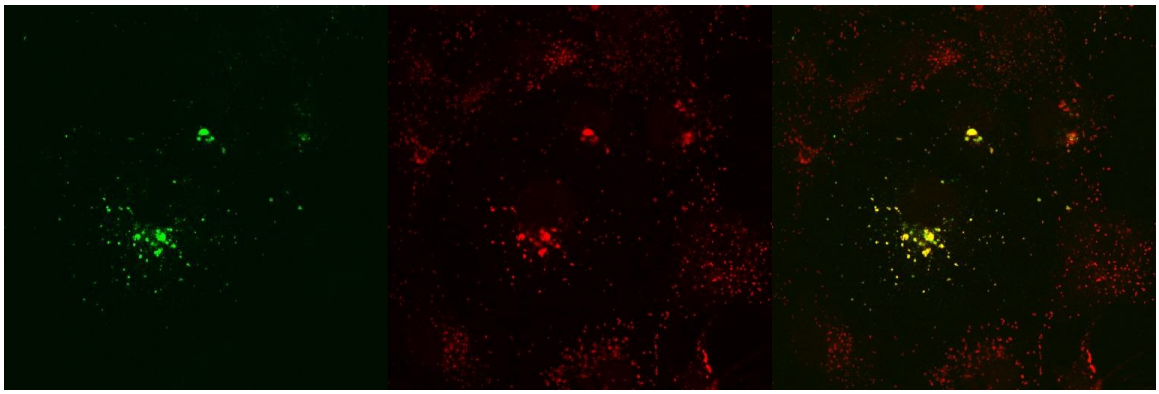

Fig. S6. COS 7 cells expressing Kaede-CD63 (green) immunostained for lamp-2 (red). The merged image (right) indicates that the two proteins largely localize to the same structures. The Kaede-CD63 expressing cells show some morphological changes compared with the non-transfected cells, which is perhaps due to overexpression of CD63. Nevertheless, these images indicate the Kaede-CD63 molecules localize to lysosomes as defined by the presence of the lysosomal membrane protein, lamp-2.

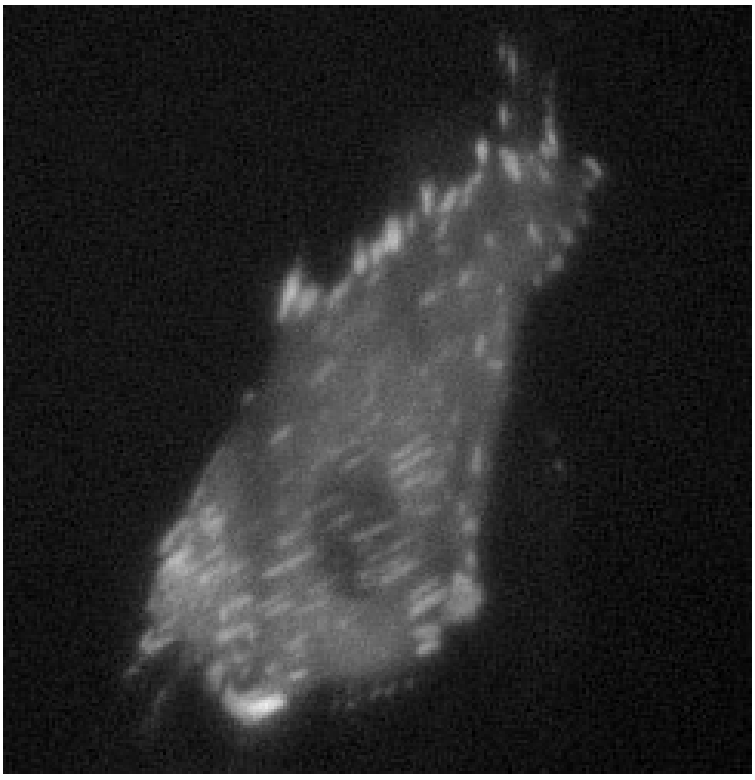

Fig. S7. A FoLu cell expressing dEosFP-tagged vinculin indicates the localization of the tagged protein at focal adhesion regions, as desired.

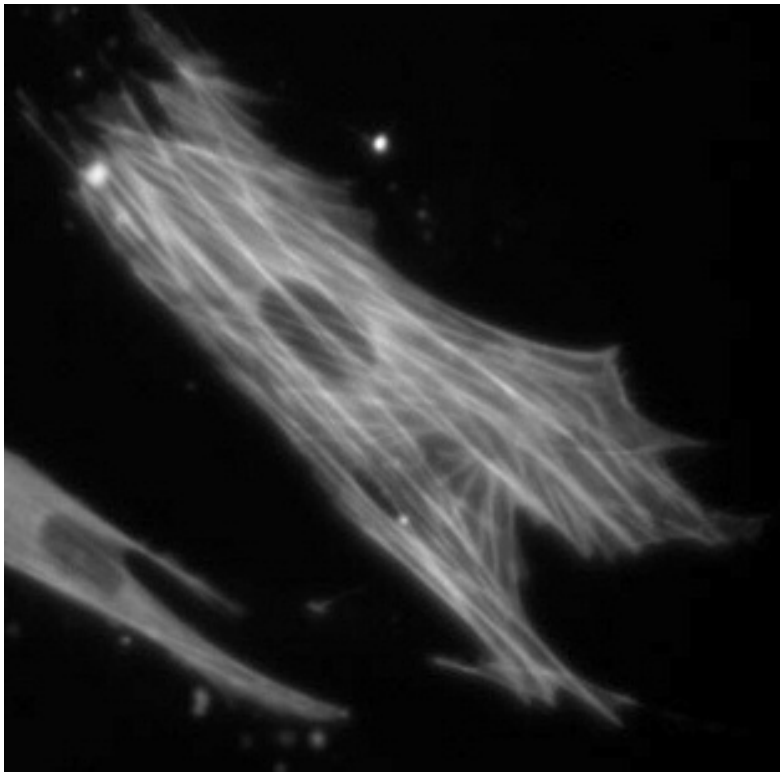

Fig. S8. FoLu cells expressing tdEosFP-tagged actin reveal the localization of the tagged protein to the actin cytoskeleton, as desired.

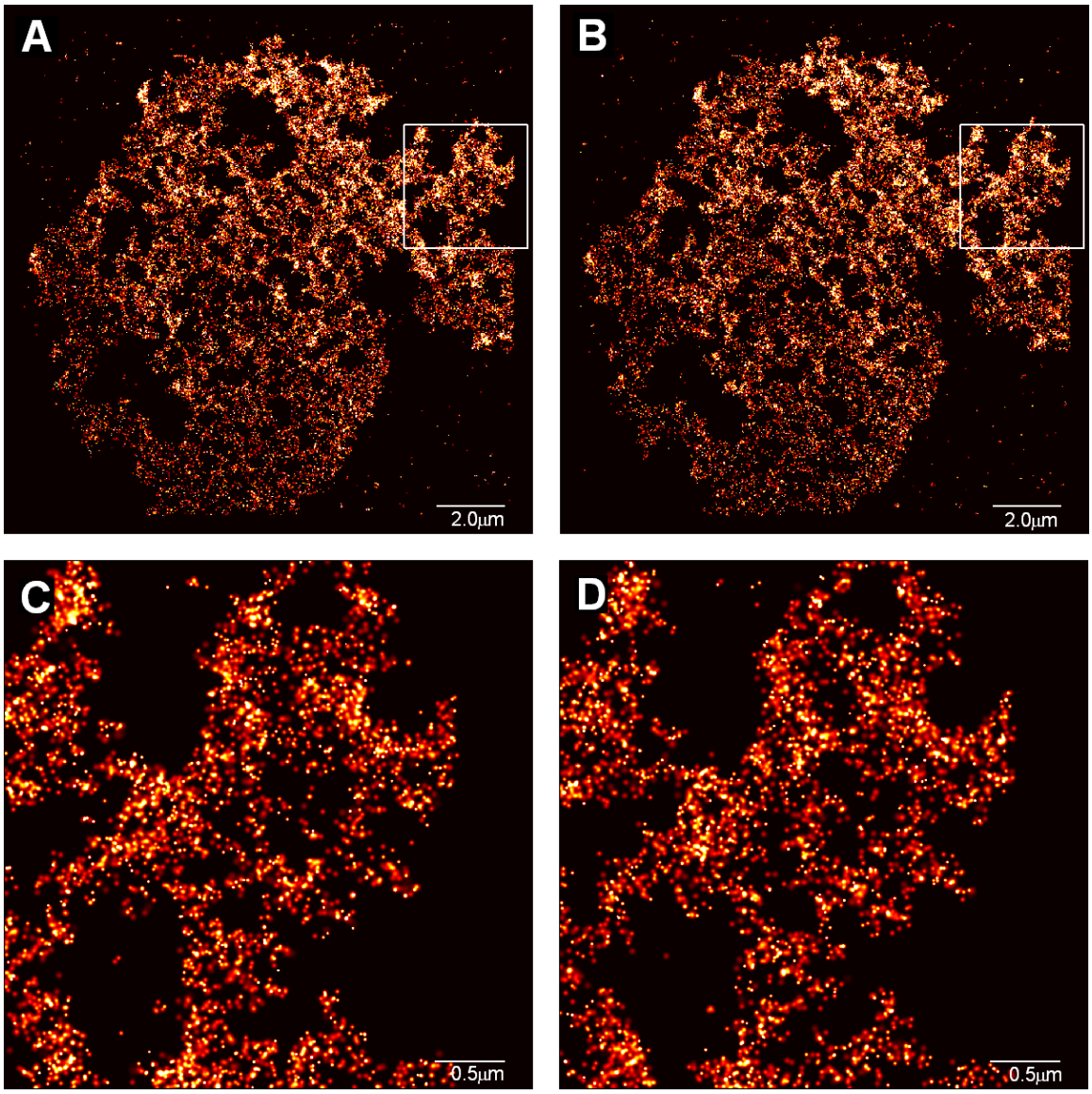

Fig. S9. PALM images of the same sample as in Fig. S3, constructed with two different subsets of activated molecules (subset 1 in (**A**) and (**C**), subset 2 in (**B**) and (**D**)). Very similar results are obtained on length scales where number of localized molecules is high ((**A**) and (**B**)), but some variability becomes evident at length scales where the individual localized molecules can be discerned ((**C**) and (**D**)).

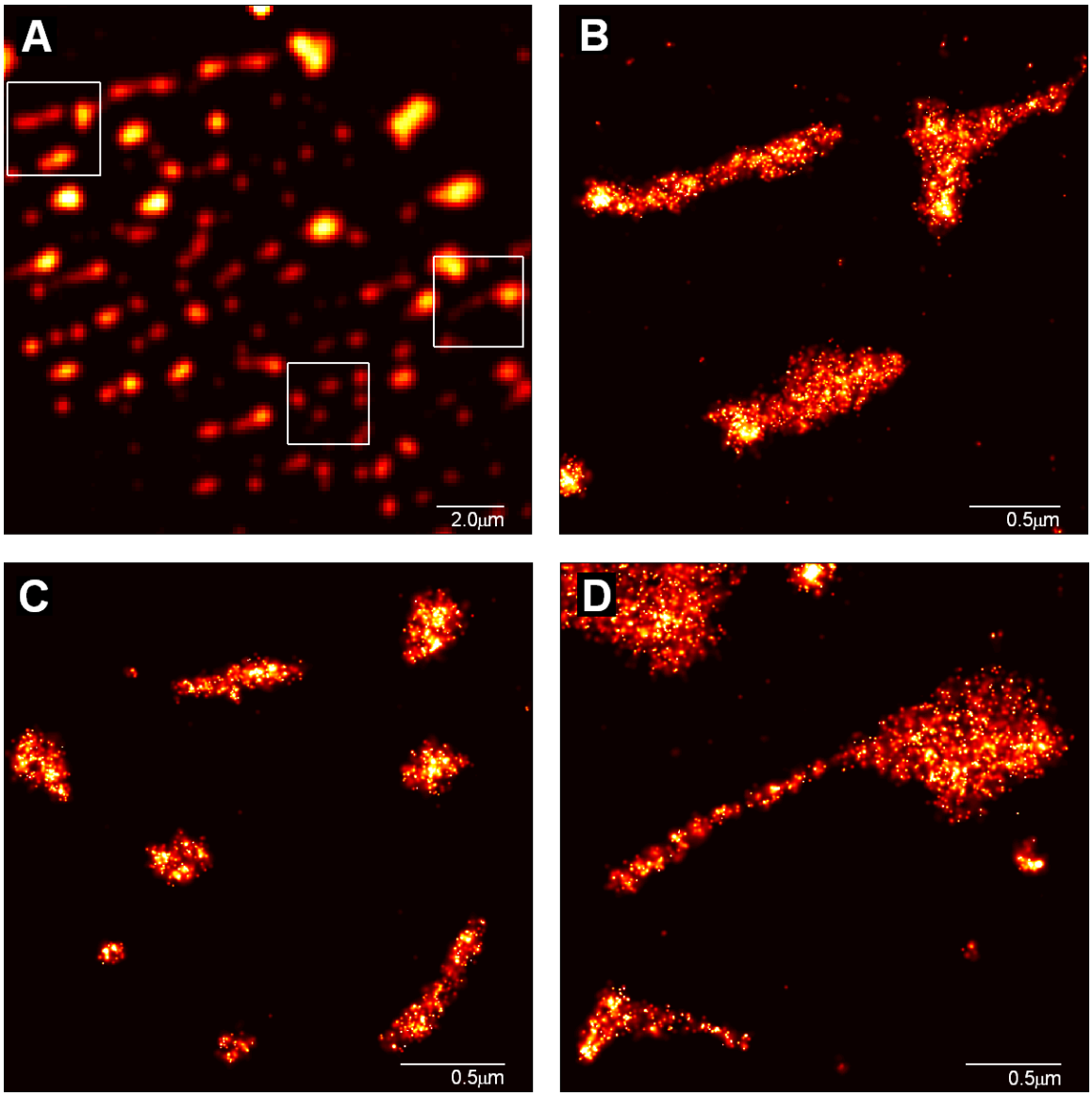

Fig. S10. (**A**) Summed TIRF and (**B** through **D**) PALM images of the regions from left to right in (**A**), obtained by photoactivation of caged rhodamine-dextran dried on a glass cover slip. Such caged dyes offer a possible alternative to PA-FPs for labeling PALM samples with high brightness, small (and thus potentially less perturbative) molecules.

ONLINE MOVIES AND ANIMATIONS

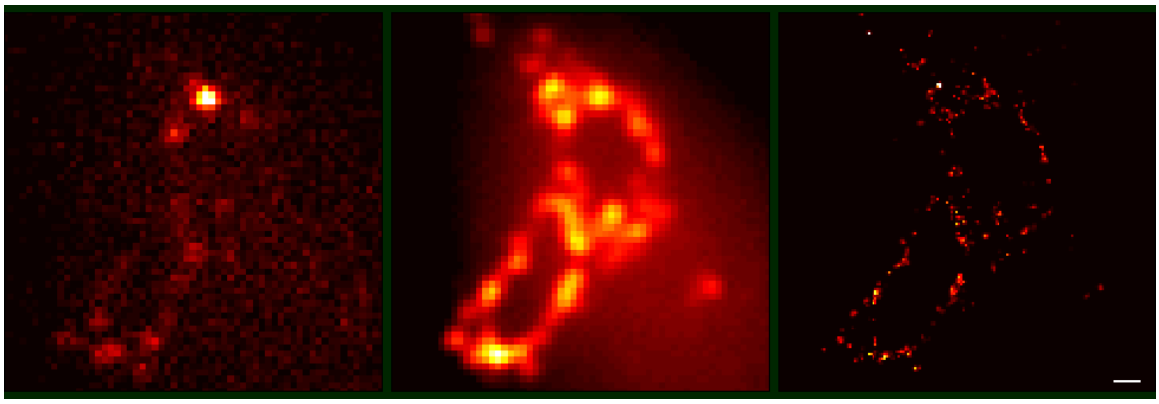

Movie S1. Partial summed molecule TIRF image (center) and PALM image (right) constructed during the acquisition of 300 single molecule frames (left) out of the 20,000 frames used to construct the images in Fig. 2. Scale bar is 0.5 μm.